Rapid downregulation of rat renal Na/P_i cotransporter in response to parathyroid hormone involves microtubule rearrangement

Marius Lötscher,[1] Yvonne Scarpetta,[1] Moshe Levi,[2] Nabil Halaihel,[2] Huamin Wang,[2] Hubert K. Zajicek,[2] Jürg Biber,[3] Heini Murer,[3] and Brigitte Kaissling[1]

[1]Institute of Anatomy, University of Zürich, CH-8057 Zürich, Switzerland
[2]University of Texas Southwestern Medical Center and Veterans Affairs Medical Center, Dallas, Texas 75216, USA
[3]Institute of Physiology, University of Zürich, CH-8057 Zürich, Switzerland

Address correspondence to: Brigitte Kaissling, Institute of Anatomy, University of Zürich, Winterthurerstr. 190, CH-8057 Zürich, Switzerland. Phone: 41-1-635-5320; Fax: 41-1-635-5702; E-mail: bkaissl@anatom.unizh.ch.

Received for publication February 26, 1998, and accepted in revised form July 7, 1999.

Renal proximal tubule cells express in their apical brush border membrane (BBM) a Na/P_i cotransporter type IIa that is rapidly downregulated in response to parathyroid hormone (PTH). We used the rat renal Na/P_i cotransporter type IIa (NaPi-2) as an in vivo model to assess early cellular events in the rapid downregulation of this transporter. When rats were treated with PTH for 15 minutes, NaPi-2 abundance in the BBM was decreased. In parallel, transporter accumulated in intracellular vesicles. Concomitantly, microtubules (MTs) were found to form dense bundles of apical-to-basal orientation. After 60 minutes of PTH action, the cells were vastly depleted of NaPi-2, whereas their microtubular cytoskeleton had returned to its normal appearance. Prevention of MT rearrangement by taxol resulted in accumulation of NaPi-2 in the subapical cell portion after 15 minutes and a strong delay in depletion of intracellular transporter after 60 minutes of PTH action. Furthermore, the subapical accumulation of NaPi-2 was associated with the expansion of dense apical tubules of the subapical endocytic apparatus (SEA). Depolymerization of MTs by colchicine likewise caused a retardation of intracellular NaPi-2 depletion.These results suggest that NaPi-2 is downregulated in response to PTH through a rapid endocytic process in 2 separate steps: (a) internalization of the transporter into the SEA, and (b) its delivery to degradative organelles by a trafficking mechanism whose efficiency depends on a taxol-sensitive rearrangement of MTs.

J. Clin. Invest. **104**:483–494 (1999).

Introduction

The epithelial cells of renal proximal tubules (PTs) express in their apical brush border membrane (BBM) a transport protein, the Na/P_i cotransporter type IIa (1), that mediates the uptake of inorganic phosphate (P_i) and sodium (Na) into the PT cells. In vivo studies on the Na/P_i cotransporter type IIa of the rat kidney (NaPi-2) have shown that this transporter is rapidly up- or downregulated at the BBM within 2 hours after acute changes in dietary P_i or treatment with parathyroid hormone (PTH) (2, 3). We have subsequently demonstrated that the rapid increase of NaPi-2 at the BBM following acute restriction of dietary P_i occurs independently of de novo protein synthesis and is sensitive to microtubule (MT) disruption by colchicine, suggesting that upregulation is mediated by MT-dependent translocation of presynthesized NaPi-2 to the BBM (4).

The rapid decrease of NaPi-2 at the BBM in response to a high dietary P_i load or PTH is accompanied by a transient increase of transporter abundance in typical intracellular regions of lysosomes before the transporter largely disappears in the PT epithelium (4, 5). Complementary studies on opossum kidney cells, which represent an established in vitro model for analyzing cellular mechanisms that control renal Na/P_i cotransport, demonstrated that treatment of the cells with PTH for 4 hours leads to a complete depletion of the intrinsic (NaPi-4) and transfected (NaPi-2) rat Na/P_i cotransporter (6). Subsequent studies on opossum kidney cells and rat kidneys pretreated with lysosomal inhibitors showed an accumulation of NaPi-2 in the typical region of lysosomes (7, 8). Additionally, recent ultrastructural investigations of rat renal PTs point to a participation of endocytic vesicles and lysosomes in the regulation of NaPi-2 (9). Together, these findings suggest that rapid downregulation of the Na/P_i cotransporter is accomplished by endocytic removal of the transporter from the BBM and its degradation in lysosomes.

In contrast to the rapid upregulation of NaPi-2, which was shown to depend on intact MTs, it is not clear whether MTs also play a role in the downregulation of the Na/P_i cotransporter. The involvement of MTs has only been determined in so far as, in response to a high dietary P_i load, the rapid decrease of NaPi-2 from the BBM was insensitive to MT disruption by colchicine (4). The significance of MT-dependent intracellular trafficking for lysosomal degradation of the Na/P_i cotransporter remains to be assessed.

In recent years, 2 other transport systems were shown to undergo similarly rapid up- and downregulation at

the plasma membrane: the insulin-stimulated glucose transporter in cells of fat and muscle tissue, GLUT-4, and the vasopressin-responsive water channel in principal cells of the renal collecting duct, AQP2, respectively (10, 11). After these transport systems have been inserted into the plasma membrane upon the specific hormone stimulus, removal of the respective hormone results in rapid internalization of GLUT-4 and AQP2, probably by constitutive endocytosis via clathrin-coated pits (12–14). Most likely, GLUT-4 and AQP2 enter the recycling pathway to be reinserted, eventually, into the plasma membrane. This transporter recycling strongly contrasts with the fate of the Na/P_i cotransporter, which is apparently degraded within a few hours in the process of downregulation. The downregulation of the Na/P_i cotransporter is, therefore, mechanistically more reminiscent of the downregulation of liganded receptors for growth factors through receptor-mediated endocytosis (RME) than any known transporter (15). In this respect, the further investigation of Na/P_i cotransporter downregulation is expected to provide insight into novel cell biological principles of transport regulation.

The purpose of this study was to reveal early cellular events in Na/P_i cotransporter downregulation that fill the mechanistic gap between transporter removal from the BBM and transporter degradation in lysosomes. More specifically, by studying the PTH-induced downregulation of the rat renal Na/P_i cotransporter, we sought to determine whether NaPi-2 is removed from the BBM by internalization into the endocytic apparatus of PT cells, from where, in analogy to RME, it would be sorted toward lysosomal degradation. Furthermore, because MTs were found to facilitate intracellular trafficking of cargo destined for lysosomal degradation (16), another target of our study was to establish if MTs play a role in steps of NaPi-2 downregulation subsequent to transporter retrieval from the BBM.

Methods

Experimental animals. The experiments were performed with male Wistar rats (150–160 g). The rats had free access to standard lab chow and tap water. Twenty-four hours before PTH treatment of rats, the drinking water was supplemented with 4% calcium heptogluconate. The higher calcium intake would lower the animals' serum level of endogenous PTH (17).

For the immunohistochemical and morphological studies on fixed kidney tissue, there were 9 experimental groups, as listed in Table 1 (groups 1–9). Each experimental group contained 3 rats; those groups with colchicine treatment contained 5 rats each. The results obtained with individual rats in each group were all consistent, except for some rats within the colchicine groups, which showed insufficient disruption of the microtubular network. These rats were excluded from further morphological interpretation. To determine BBM Na/P_i cotransport activity, and for Western blot analysis of renal cortical homogenate fractions, 9 groups of 4 rats each were studied (Table 1, groups 10–18).

Taxol, colchicine, and PTH treatment of rats. Taxol (paclitaxel) lyophilisate (Sigma Chemical Co., St. Louis, Missouri, USA) was dissolved in DMSO at 5 mg/mL. The taxol solution was injected intraperitoneally 8 hours and 3 hours before surgery for PTH treatment and perfusion, at a dosage of 5 mg/kg body weight. Colchicine (Sigma Chemical Co.) was dissolved in saline, and a dose of 1 mg/kg body weight was injected intraperitoneally 6 hours before surgery. Rats of groups 1, 2, 3, 10, 11, 12, 13, and 14 (Table 1) underwent the same treatment with the vehicles (DMSO and saline) alone.

Lyophilisate of rPTH 1-34 (peptide content 73%; Bachem AG, Bubendorf, Switzerland) was reconstituted at 0.5 mg/mL in a solution of 10 mM acetic acid, 0.4 mM DTT, and 1% BSA. Rats were anesthetized with thiopental (Pentothal; 100 mg/kg body weight) injected intraperitoneally, and their abdominal cavities were prepared for perfusion fixation as described elsewhere (18). PTH was injected into the vena cava as a single bolus of 100 μg (active peptide)/kg body weight, diluted to a volume of 250 μL with 0.9% saline. Rats of groups 1, 4, 7, 10, 13, 15, and 17 (Table 1) received an intravenous injection of vehicle alone.

BBM isolation. At 15, 30, or 60 minutes after injection of PTH (or vehicle), the kidneys designated for BBM isolation were removed from the anesthetized rats. The superficial cortex was dissected and homogenized in 15 mL of an isolation buffer consisting of 300 mM mannitol, 5 mM EGTA, 1 mM PMSF, 16 mM HEPES, and 10 mM Tris (pH 7.5). An aliquot of the cortical homogenate was saved for subsequent Western blot analysis. BBMs were isolated from this homogenate by Mg^{2+} precipitation and differential centrifugation as described previously (19). The resulting BBM pellet was resuspended in a buffer of 300 mM mannitol, 16 mM HEPES, 10 mM Tris (pH 7.5) and was aliquoted for transport measurements and Western blotting.

BBM transport measurements. Transport measurements were performed in freshly isolated BBM vesicles by radiotracer uptake followed by rapid millipore filtration. To measure Na^+ gradient–dependent $^{32}P_i$ uptake (Na/P_i cotransport), 10 μL of BBM preloaded in an intravesicular buffer of 300 mM mannitol, 16 mM HEPES, and 10 mM Tris (pH 7.5) was vortex mixed at 25°C with 40 μL of an extravesicular uptake buffer of 150 mM NaCl, 100 μM

Table 1
Experimental groups of rats and their treatment

Experimental group	Antimitotic drug	PTH
1, 10	–	–
2, 11	–	15 minutes
3, 12	–	60 minutes
4	Colchicine	–
5	Colchicine	15 minutes
6	Colchicine	60 minutes
7	Taxol	–
8	Taxol	15 minutes
9	Taxol	60 minutes
13	–	–
14	–	30 minutes
15	Colchicine	–
16	Colchicine	30 minutes
17	Taxol	–
18	Taxol	30 minutes

Groups 1–9 were set up for immunohistochemistry; groups 10–18 were set up for transport studies and Western blot analysis.

$K_2H^{32}PO_4$, 16 mM HEPES, and 10 mM Tris (pH 7.5). Uptake after 10 seconds (representing initial linear rate) was terminated by an ice-cold stop solution. All uptake measurements were performed in triplicate, and uptake was calculated on the basis of specific activity determined in each experiment and expressed as pmol/10 s/mg BBM protein.

SDS-PAGE and immunoblotting. Samples of BBM and cortical homogenate were denatured for 2 minutes at 95°C in 2% SDS, 10% glycerol, 0.5 mM EDTA, and 95 mM Tris-HCl (pH 6.8, final concentrations). Ten micrograms BBM and 20 μg cortical homogenate protein per lane were separated on 9% polyacrylamide gels and electrotransferred onto nitrocellulose paper. After blockage with 5% nonfat milk powder with 1% Triton X-100 in Tris-buffered saline (20 mM, pH 7.3), Western blots were incubated with antiserum against NaPi-2 (20) at a dilution of 1:4,000. Primary antibody binding was viewed using enhanced chemiluminescence (Pierce Chemical Co., Rockford, Illinois, USA), and the signals were quantitated in a PhosphorImager with chemiluminescence detector and densitometry software (Bio-Rad Laboratories Inc., Richmond, California, USA).

Tissue fixation. At the end of the PTH treatment period, the kidneys designated for immunohistochemical and morphological studies were fixed by retrograde perfusion of the anesthetized rats through the abdominal aorta at a pressure of 1.38 hp. The fixative was composed of 3% paraformaldehyde and 0.05% picric acid in a 6:4 mixture of 0.1 M cacodylate buffer (pH 7.4, adjusted to 300 mOsm with sucrose) and 10% hydroxyethyl starch in saline (HAES steril; Fresenius AG, Bad Homburg, Germany). After 5 minutes of fixation, the fixative was replaced by perfusion for 5 minutes with cacodylate buffer.

Immunohistochemistry. Coronal slices of fixed kidneys were snap-frozen in liquid propane cooled by liquid nitrogen. Sections 3-μm thick were cut at –22°C in the cryomicrotome, mounted on chrome alum/gelatin-coated glass slides, thawed, and stored in cold PBS buffer until used.

For NaPi-2/α-tubulin, NaPi-2/58K, and NaSi-1/F-actin immunofluorescence staining, sections were preincubated for 5 minutes at room temperature with 3% milk powder in PBS containing 0.05% Triton X-100. They were covered overnight at 4°C with primary antibodies diluted in preincubation solution. Dilutions were 1:500 for rabbit antisera against NaPi-2 (20) and NaSi-1 (21), and 1:1,000 for monoclonal mouse antibodies (Sigma Chemical Co.) against α-tubulin and 58K. The sections were rinsed 3 times with PBS before incubation for 1 hour at 4°C with the secondary antibodies swine anti-rabbit IgG conjugated to FITC (DAKO A/S, Glostrup, Denmark) and goat anti-mouse IgG conjugated to Cy3 (Jackson ImmunoResearch Laboratories Inc., West Grove, Pennsylvania, USA) or phalloidin-rhodamine (Molecular Probes Inc., Eugene, Oregon, USA), diluted 1:50, 1:200, and 1:100, respectively, in preincubation solution.

After being rinsed with PBS, the sections were mounted using DAKO-Glycergel (DAKO A/S) plus 2.5% 1,4-diazabicyclo{2.2.2}octane (DABCO; Sigma Chemical

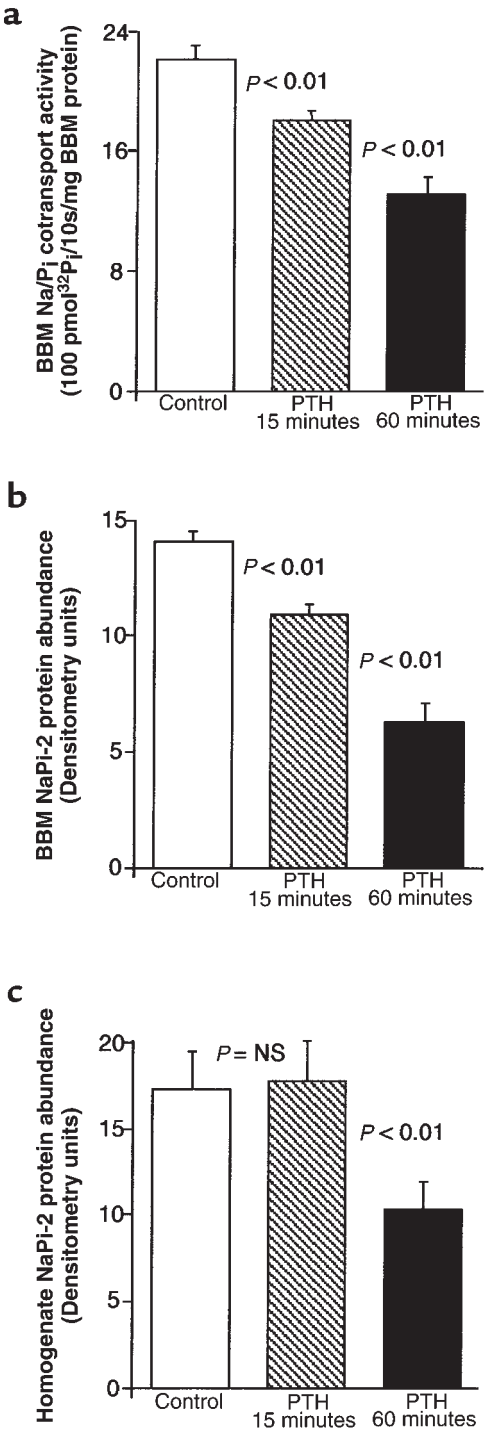

Figure 1
Effect of PTH on Na/P_i cotransport activity and NaPi-2 protein abundance. (**a**) Transport activity was determined by measurement of Na^+-dependent P_i uptake into BBM vesicles. After 15 minutes of treatment with PTH, there is a significant decrease in transport activity, which is further pronounced after 60 minutes of PTH. (**b** and **c**) Western blots of BBM or total cortical homogenate samples were immunoprobed for NaPi-2 protein, and the chemiluminescent signals were quantitated densitometrically. Like transport activity, NaPi-2 protein abundance at the BBM is already decreased after 15 minutes of PTH (**b**). Total NaPi-2 protein abundance in the cortical homogenate, however, is not significantly altered after this time period (**c**). After 60 minutes, both BBM and homogenate NaPi-2 are substantially decreased.

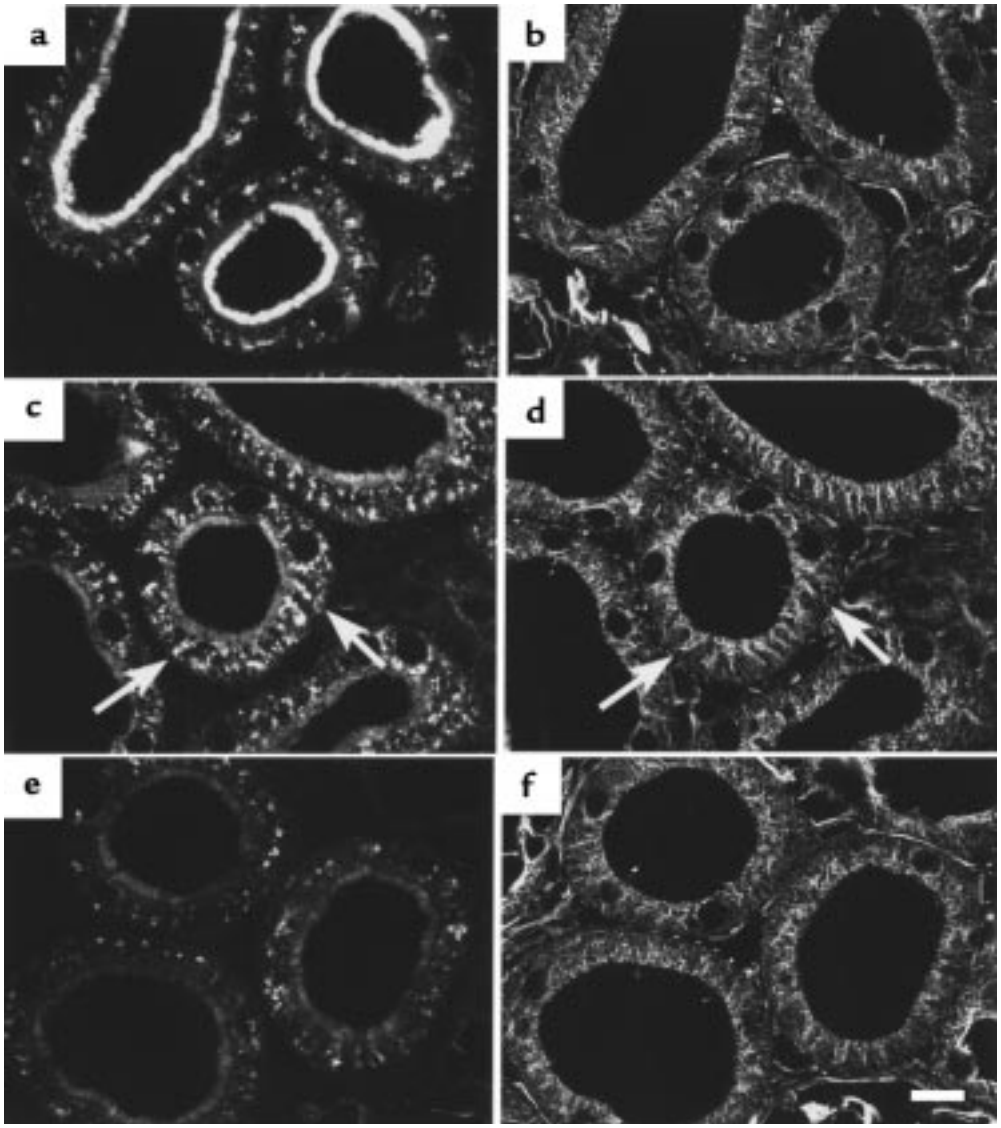

Figure 2
PTH-induced downregulation of NaPi-2 and concomitant rearrangement of MTs. Rats were treated with vehicle (**a** and **b**), PTH for 15 minutes (**c** and **d**), or PTH for 60 minutes (**e** and **f**). Cryosections showing PTs in the superficial cortex were immunofluorescently double-stained for NaPi-2 (**a**, **c**, and **e**) and α-tubulin (**b**, **d**, and **f**). In PTs of control (vehicle-injected) rats, NaPi-2 is predominantly detected in the luminal brush border. Intracellular NaPi-2 staining is confined mainly to the juxtanuclear region. Staining of α-tubulin depicts MTs forming a fine network with higher density in the apical cell portion. After 15 minutes of PTH, brush border NaPi-2 is decreased, whereas a great number of intracellular vesicles are loaded with transporter (**c**). MTs have partially rearranged to form dense bundles with apical-to-basal orientation (**d**). The bundles spatially coincide with the arrayed NaPi-2–containing vesicles (arrows). After 60 minutes of PTH, NaPi-2 has disappeared. The microtubular cytoskeleton has rearranged to look as it did under control conditions. Scale bar: 10 μm.

Co.) as a fading retardant. They were studied with a laser scanning microscope (Zeiss, Oberkochen, Germany) by confocal fluorescence imaging.

Electron microscopy. From each fixed kidney, small tissue blocks comprising superficial cortex were immersed overnight in the same fixative as described above, to which 0.5% glutaraldehyde was added. After osmification in 1% OsO_4 for 30 minutes, the tissue was embedded into epoxy resin, according to routine procedures. Ultrathin sections of 60 nm were cut with an ultramicrotome (Reichert-Jung, Vienna, Austria) and stained with lead citrate and uranyl acetate. The sections were examined on a Phillips CM 100 electron microscope.

Statistical analysis. All data were expressed as mean ± SEM. A 2-tailed unpaired Student's *t* test and/or a 1-way ANOVA with Student-Newman-Keuls multiple range test was used to compare results between experimental groups. Significance was accepted at $P < 0.05$.

Results

Our method of injecting PTH intravenously into anesthetized rats allowed us to perform the hormone treatment for periods as short as 5 minutes and, without noticeable side effects from anesthesia, as long as 60 minutes. Initial immunohistochemical evaluation of the PTH effect at various time points (i.e., 5, 10, 15, 20,

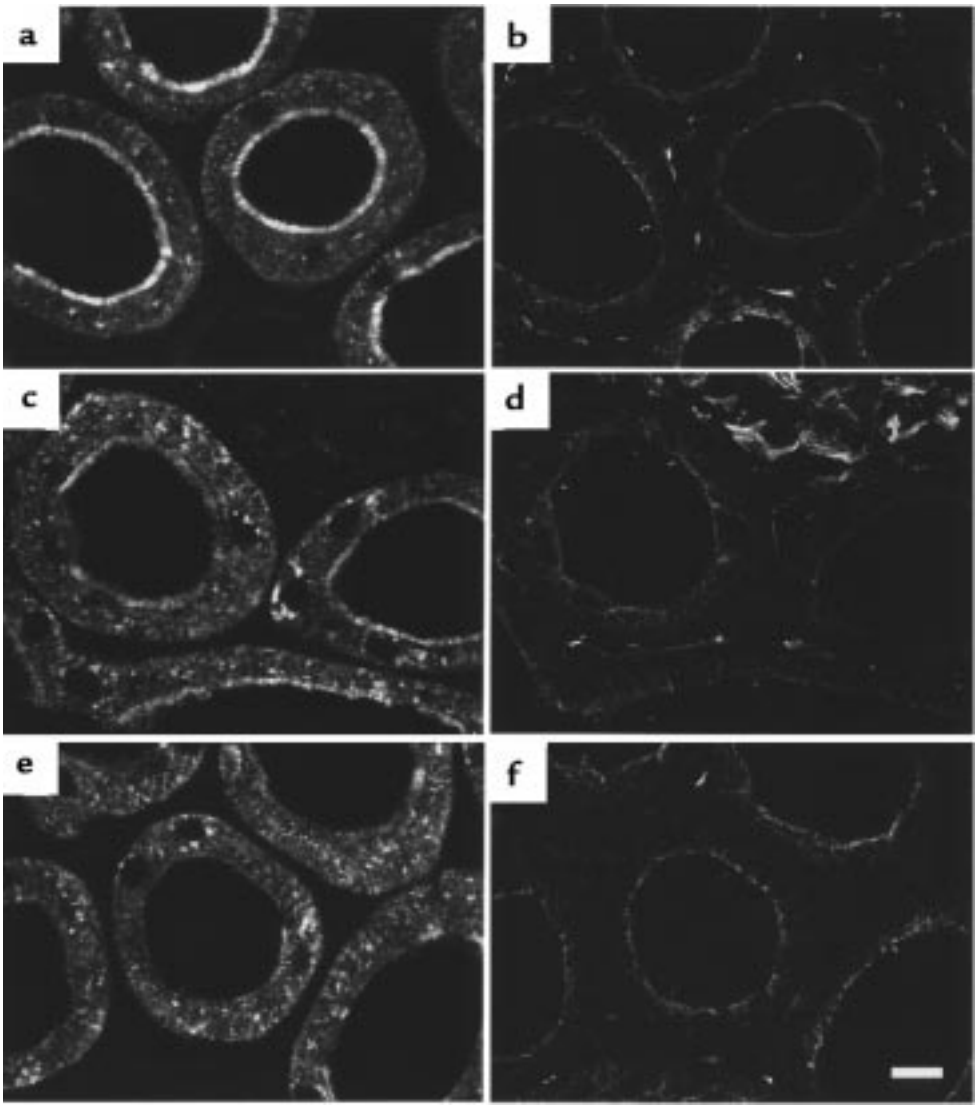

Figure 3
Effect of MT disruption by colchicine on PTH-induced downregulation of NaPi-2. After colchicine pretreatment, rats were treated with vehicle (**a** and **b**), PTH for 15 minutes (**c** and **d**), or PTH for 60 minutes (**e** and **f**). Cryosections showing PTs in the superficial cortex were immunofluorescently double-stained for NaPi-2 (**a**, **c**, and **e**) and α-tubulin (**b**, **d**, and **f**). Colchicine pretreatment per se not only causes a vast disappearance of the MT network, but also affects the localization of NaPi-2 protein in PT cells. BBM expression appears to be lowered, whereas intracellular transporter has lost its defined compartmentalization (**a**). Nonetheless, PTH-induced NaPi-2 downregulation at the BBM seems to proceed normally. On the other hand, depletion of intracellular transporter after 60 minutes of PTH is not observed (**e**). Scale bar: 10 μm.

30, 45, and 60 minutes after injection) had shown that the onset of NaPi-2 downregulation at the BBM was already faintly detectable after 5 minutes and was very pronounced after 15 minutes. Downregulation at the BBM was found to proceed continually, though with only little difference detectable between 45 and 60 minutes. Intracellular depletion became clearly detectable immunohistochemically after 30 minutes, being very striking after 60 minutes. Based on these preliminary immunohistochemical findings and considering the number of required experimental animals, the transport measurements, Western blot analysis of membrane fractions, and morphological examinations of aldehyde-fixed kidney tissue focused on the time points of 15 and 60 minutes (or just 30 minutes in a follow-up series of experiments as seen below).

Rapid downregulation of P_i transport activity and NaPi-2 protein abundance in response to PTH. The Na/P_i cotransport activity, as measured on isolated BBM vesicles, was clearly decreased 15 minutes after treatment of rats with PTH (Figure 1a). By 60 minutes, the decrease had more than doubled. The PTH-induced downregulation of transport activity was reflected by a corresponding decrease of NaPi-2 protein abundance in the BBM fraction of cortical homogenate (Figure 1b). A different time course, however, was found for total NaPi-2 protein abundance in nonfractionated cortical homogenate (Figure 1c): after 15 minutes of PTH, transporter abundance was still on the level of nontreated controls, whereas a strong decrease was seen only at the 60-minute time point. These results suggest that PTH-induced downregulation of transport activity is achieved initially by a rapid redistribution of NaPi-2

protein from the BBM to different membrane sites, which is then followed by a depletion of the transporter. To get insight into underlying intracellular events, immunohistochemical studies were performed.

Immunohistochemical localization of NaPi-2 in PT cells of control rats. Cryosections of rat kidneys were immunohistochemically stained using a specific antiserum directed against NaPi-2 (20). In kidneys of control rats, the transporter was found to be highly expressed in the brush border of the PT epithelium (Figure 2a). Furthermore, NaPi-2 was detected in intracellular compartments that were predominantly located in the vicinity of cell nuclei. Most of the perinuclear NaPi-2 colocalized with the Golgi region marker protein 58K (4, 22). The significance of intracellular NaPi-2 in the Golgi-like region is unknown.

Structure of MTs in PT cells of control rats. The cryosections used for NaPi-2 localization were costained with antibodies directed against α-tubulin in order to reveal the morphology of the microtubular cytoskeleton. As shown in Figure 2b, MTs formed a dense network through the entire PT cell, except for the brush border, where only single cilium were occasionally apparent. The cell-spanning network was not uniform, but exhibited typical features of the microtubular cytoskeleton of polarized epithelial cells (23): in most cells, the network was densest in the apical portion, the region where the MT organization centers are also located. In addition, most MTs were oriented in an apical-to-basal axis.

Effect of PTH on subcellular NaPi-2 localization and MT arrangement. Treatment of rats with PTH altered both the localization of NaPi-2 and the structure of MTs in

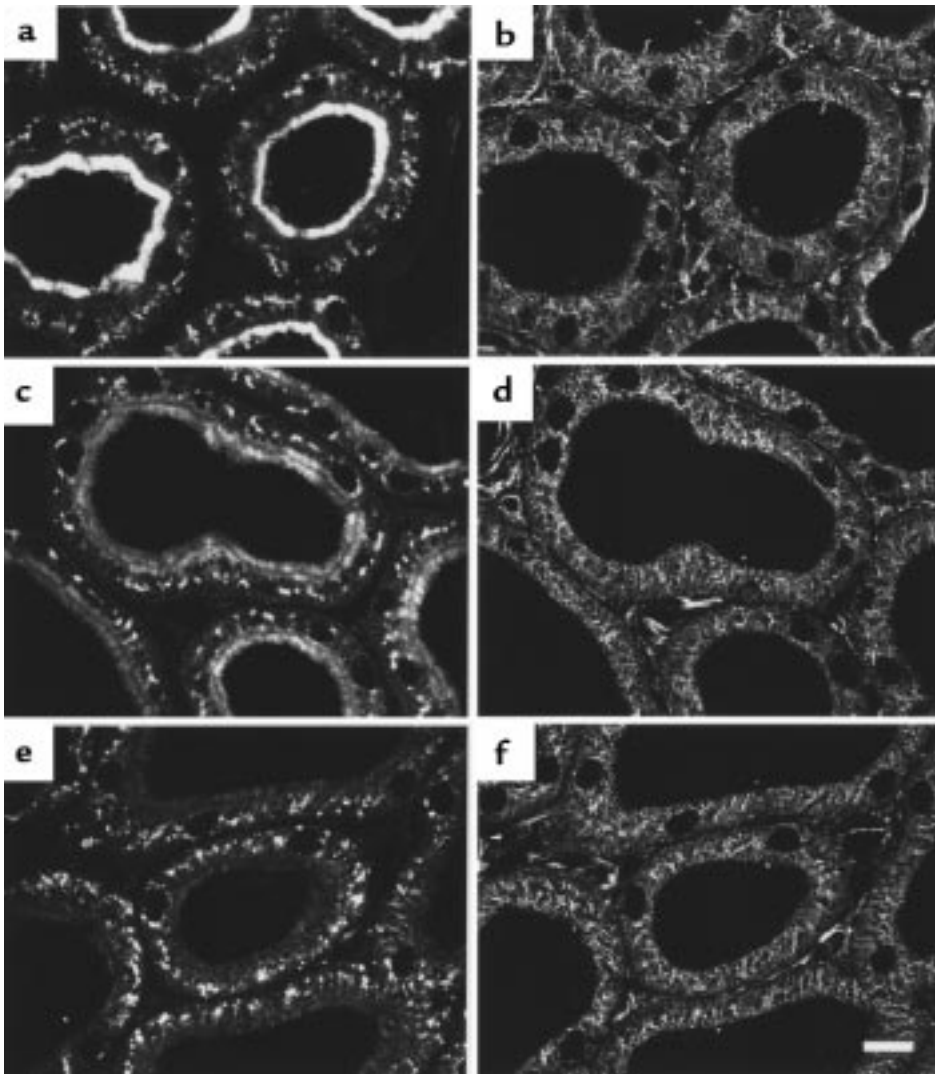

Figure 4
Effect of MT stabilization by taxol on PTH-induced downregulation of NaPi-2. After taxol pretreatment, rats were treated with vehicle (**a** and **b**), PTH for 15 minutes (**c** and **d**), or PTH for 60 minutes (**e** and **f**). Cryosections showing PTs in the superficial cortex were immunofluorescently double-stained for NaPi-2 (**a**, **c**, and **e**) and α-tubulin (**b**, **d**, and **f**). Taxol pretreatment per se has no manifest effect on the expression of NaPi-2. Likewise, the microtubular cytoskeleton appears as it does under control conditions. PTH treatment of taxol-pretreated rats for 15 minutes causes a decrease of brush border NaPi-2. In parallel, a subapical region of about the same extension as the brush border has accumulated the transporter (**c**). Rearrangement of MTs seems to be successfully prevented by taxol (**d**). PTH treatment of taxol-pretreated rats for 60 minutes leads to nearly complete NaPi-2 depletion in the brush border, although intracellular vesicles still contain NaPi-2 in abundance (**e**). Scale bar: 10 μm.

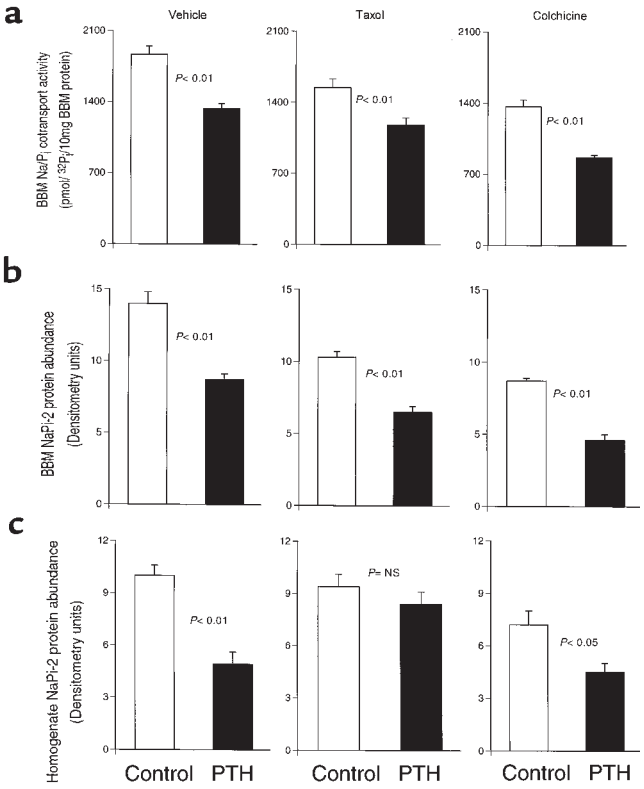

Figure 5
Taxol and colchicine effects on PTH-induced downregulation of Na/P_i cotransport, as determined by measurement of BBM transport activity (**a**) and Western blot analysis of NaPi-2 protein abundance in the BBM fraction (**b**) and total homogenate (**c**). Pretreatment of rats with vehicle, taxol, or colchicine was followed by mock or PTH treatment for 30 minutes. Transport activity is decreased upon PTH treatment, irrespective of pretreatment with antimitotic drugs. Likewise, PTH-induced depletion of NaPi-2 protein in the BBM fraction seems to be unaffected by taxol or colchicine. NaPi-2 protein abundance in total homogenate, however, is only insignificantly decreased after 30 minutes of PTH, when rats have been pretreated with taxol. Colchicine seems to perturb this depletion of NaPi-2 protein in the homogenate, too, albeit less efficiently.

PT cells. In accordance with the results from Western blot analysis, NaPi-2 abundance was decreased in the brush border 15 minutes after PTH injection (Figure 2c). In parallel, considerably more intracellular NaPi-2 was detected, located in large vesicular organelles that frequently were arrayed in an apical-to-basal orientation. At the same time, the microtubular cytoskeleton had altered its morphology: MTs were arranged in dense bundles converging from the apical toward the basal cell pole (Figure 2d). Arrays of NaPi-2–containing vesicles appeared to be aligned along these MT bundles.

In kidneys of rats treated with PTH for 60 minutes, the brush border of PT cells was vastly depleted of NaPi-2 (Figure 2e). In intracellular compartments, where NaPi-2 was very abundant after 15 minutes of PTH, the transporter also had largely disappeared. Only in a few vesicular organelles in the basal cell portion was NaPi-2 still detected. Again, these immunohistochemical findings for NaPi-2 are in accordance with the Western blot data. The appearance of the microtubular cytoskeleton after 60 minutes of PTH (Figure 2f) was similar to what was seen in kidneys of control rats, indicating that the formation of MT bundles observed at 15 minutes of PTH treatment was only transient.

Effect of colchicine treatment on rapid NaPi-2 downregulation. The coincident occurrence of the intracellular redistribution of NaPi-2 protein and an MT rearrangement upon PTH treatment imply that MTs might play a role in the rapid downregulation of the transporter. To test this hypothesis, rats were pretreated with the MT-depolymerizing drug colchicine. Colchicine dosage was kept low and the exposure time short, in order to minimize undesired systemic effects. As a putative consequence, some rats exhibited only a partial disruption of the MT network in PT cells, as assessed by immunohistochemistry. These rats were excluded from further morphological interpretation. Figure 3, b, d, and f, illustrates the ample disruption of MTs by the action of colchicine, leaving only some MT remnants, predominantly in the apical cell portion.

In the absence of an intact MT network, intracellular NaPi-2 protein appeared vastly dispersed throughout PT cells (Figure 3a). This was likely due to the loss of MT-dependent positioning of cytoplasmic membrane compartments. The depletion of NaPi-2 protein in the BBM in response to PTH was, in accordance with related experiments with dietary P_i (4), not notably affected by colchicine. After 15 minutes of PTH, the decrease of the transporter in the BBM was paralleled by an increase of its intracellular abundance, as in the absence of colchicine. However, this increase could not be morphologically assigned to any intracellular compartment (Figure 3c). Interestingly, intracellular NaPi-2 protein seemed not to be markedly depleted after 60 minutes of PTH when MTs were disintegrated by colchicine (Figure 3e). These findings may indicate that MTs are not necessary for the rapid redistribution of NaPi-2 protein from the BBM to intracellular sites, but that they are crucially involved in efficient transporter degradation.

Interference of taxol with PTH effects. The colchicine experiments provided strong evidence that efficient NaPi-2 protein depletion in PT cells in response to PTH is dependent on intact MTs. However, the vast loss of intracellular compartmentalization upon MT disintegration did not allow

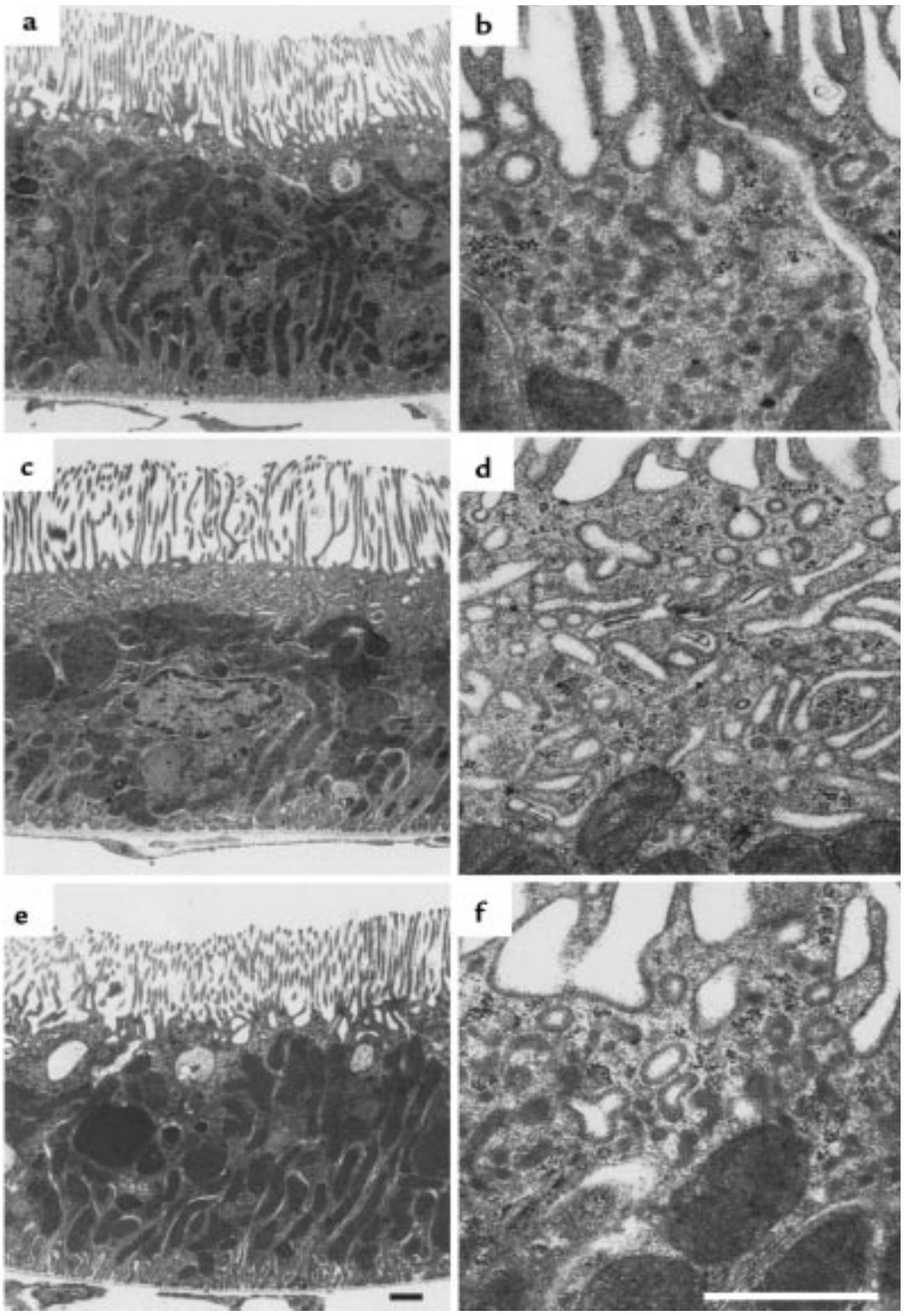

Figure 6
Morphological alteration in the subapical region of PT cells after taxol and PTH treatment. Electron microscopy images of ultrathin Epon sections show at lower (**a**, **c**, and **e**) and higher (**b**, **d**, and **f**) magnification a subapical zone in PT cells that is free of large, electron-dense organelles. (**a** and **b**) In control rats, this zone is of variable extension and is morphologically predominated by small profiles of DATs. (**c** and **d**) If taxol-pretreated rats are treated with PTH for 15 minutes, establishing conditions that lead to accumulation of NaPi-2 in the subapical region, many PT cells exhibit an expanded subapical zone containing numerous large membrane profiles of tubular and branched shape. (**e**) Treatment of rats solely with taxol does not cause morphological changes in the subapical region. (**f**) Sixty minutes after PTH injection into taxol-pretreated rats, the subapical region has returned to its normal appearance, with numerous DATs. Scale bars: 1 μm.

further morphological dissection of the downregulatory mechanisms. Moreover, the significance of the observed transient rearrangement of MTs into bundles (Figure 2d) could not be investigated by the MT-depolymerizing drug. Therefore, we instead pretreated rats with taxol (paclitaxel), an antimitotic drug that stabilizes the MT network by preventing MT depolymerization. The treatment with taxol per se did not have any apparent effect on NaPi-2 expression or microtubular morphology (Figure 4, a and b). Likewise, taxol treatment did not noticeably affect the PTH-induced decrease of NaPi-2 in the BBM (Figure 4, c and e). However, taxol given before PTH treatment completely prevented the formation of MT bundles: no alterations in the morphology of the microtubular cytoskeleton were detected 15 minutes and 60 minutes after PTH treatment (Figure 4, d and f).

Besides the stabilization of the MT network, taxol treatment had a striking effect on the intracellular localization of NaPi-2. At 15 minutes of PTH treatment, NaPi-2 accumulated in a distinct subapical zone that was clearly delimited from the brush border (Figure 4c). The increase of intracellular NaPi-2 in numerous large vesicles, as found in the absence of taxol, was lacking. Hence, inhibition of MT rearrangement by taxol is apparently associated with aberrant or declined trafficking of rapidly internalized NaPi-2 protein.

At 60 minutes of PTH treatment, NaPi-2 had disappeared again in the subapical zone. Instead, the transporter was abundantly detected in dispersed vesicular organelles (Figure 4e), as it was in non–taxol-treated rats after 15 minutes of PTH. Thus, regarding NaPi-2 depletion of PT cells after 60 minutes of PTH, taxol seemed to act as an inhibitor, like colchicine.

Transport measurements and Western analysis confirm immunohistochemical findings. To obtain transport and Western blot data complementary to the immunohistochemical findings on the effect of taxol and colchicine, rats were pretreated with the antimitotic drugs or the corresponding vehicles and then either mock or PTH treated for 30 minutes. Neither taxol nor colchicine significantly perturbed the rapid PTH-induced downregulation of Na/P_i cotransport or NaPi-2 protein abundance in the BBM (Figure 5, a and b). Analysis of total cortical homogenate revealed that the depletion of NaPi-2 protein within 30 minutes of PTH was virtually blocked by taxol, whereas colchicine appeared to inhibit this depletion only in part (Figure 5c). The latter finding for colchicine does not conform with the corresponding immunohistochemical result of cellular transporter depletion being hardly detectable, even after 60 minutes of PTH. This inconsistency might be due to the variability in the degree of MT disruption among colchicine-treated rats. In the case of Western blot analysis, efficiency of the colchicine treatment could not be premonitored, as in the immunohistochemical studies. Apart from this seeming discrepancy, the transport, Western blot, and immunohistochemical data are all consistent with each other.

Ultrastructural alterations in the subapical region of PT cells. Besides indicating that MTs, and in particular, an MT rearrangement, play a crucial role in PTH-induced NaPi-2 downregulation, the taxol results also revealed an unusual accumulation of internalized NaPi-2 protein in the subapical region of PT cells, before the evident retardation in NaPi-2 deprivation. To identify subapical compartment(s) involved in normal or taxol-perturbed transporter downregulation, samples from the same kidney tissue used for immunofluorescence staining were embedded in epoxy resin and processed for morphological examination of the PT cells by electron microscopy.

The subapical compartment comprises the so-called endocytic apparatus. It includes clathrin-coated invaginations of the apical membrane, cisternae, and dense apical tubules (DATs). The cisternae and the DATs form a largely continuous network in the apical cell pole and are associated with sorting and recycling of endocytic

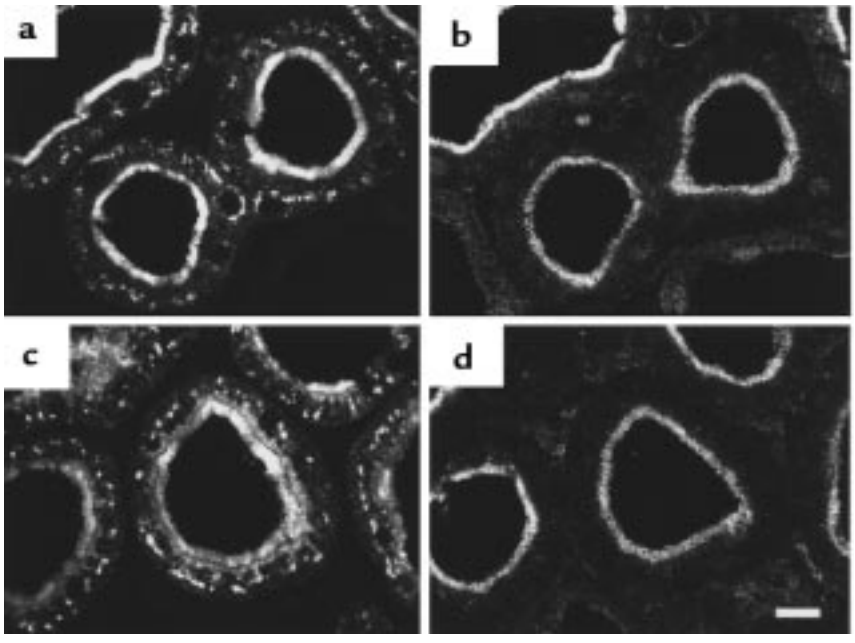

Figure 7
Absence of a PTH effect on NaSi-1. After taxol pretreatment, rats were treated with vehicle (**a** and **b**) or PTH for 15 minutes (**c** and **d**). Consecutive cryosections showing PTs in the superficial cortex were immunofluorescently stained for NaPi-2 (**a** and **c**) and NaSi-1 (**b** and **d**). In rats treated solely with taxol (and vehicle), the brush border localization of both transporters is evident. After PTH treatment for 15 minutes, NaPi-2 has decreased in the brush border and accumulated in the subapical region. In contrast, NaSi-1 is apparently unaffected by this treatment. Scale bar: 10 μm.

cargo and receptors. They reveal a coat with a characteristic substructure at their luminal side, whereas their cytoplasmic face is uncoated. Occasionally, the DATs carry small clathrin-coated buds (24–26).

Under control conditions, the subapical zone appeared as an irregular narrow band that contained numerous, more or less deep invaginations (Figure 6a) and abundant DATs (Figure 6b).

Treatment with taxol alone had no effect on the morphology of the subapical region (Figure 6e). However, when taxol treatment was followed by PTH treatment for 15 minutes, the morphology of the subapical zone of many PT cells was strikingly altered. It appeared as a broad band of regular width (Figure 6c) that contained numerous large, elongated membrane profiles, some of which were branched or anastomosing (Figure 6d) and which were preferentially arranged more or less parallel to the apical surface. These membrane profiles revealed on the luminal face the characteristic coat of DATs and lacked a clathrin coat at the cytoplasmic face. Small clathrin-coated vesicles were occasionally interspersed among the expanded tubules. Because the characteristic small profiles of DATs became rare with the appearance of the large-profile membrane tubules, we assumed that the latter represented an expanded form of the DATs. After 15 minutes of PTH, but in the absence of taxol, a similar expansion of DATs was occasionally detected in a few PT cells. The incidence of this phenomenon was significant, albeit much lower than after taxol pretreatment.

By 60 minutes after PTH treatment, irrespective of taxol pretreatment, the morphology of the subapical region appeared as it did under control conditions (Figure 6f), indicating that the morphological changes observed after 15 minutes of PTH were transient.

Specificity of the taxol/PTH effect. The PTH-induced downregulation of NaPi-2 in taxol-pretreated rats was accompanied by such striking alterations in PT cells that the question of specificity of the cell response arose. Under these conditions, therefore, we studied the expression of another transporter in the BBM of rat PT cells, the Na^+-dependent sulfate transporter NaSi-1 (21). In contrast to NaPi-2, NaSi-1 abundance and localization were found to be unaffected by PTH treatment in both non–taxol-treated (5) and taxol-treated rats (Figure 7). Similarly, staining of actin filaments (which constitute the cytoskeleton of the brush border microvilli) with rhodamine-conjugated phalloidin depicted no alterations in the microfilamentous cytoskeleton upon treatment with taxol and PTH. These findings provide strong evidence that the described cell responses are specifically associated with the rapid downregulation of NaPi-2.

Discussion

In the present study, we demonstrate rapid and specific downregulation of NaPi-2 by PTH at the apical BBM of rat renal PT cells, a simultaneous transient increase of the transporter at intracellular sites, and, ultimately, depletion of the transporter from the cells. These data strongly suggest that the downregulation of NaPi-2 in response to PTH occurs through endocytosis of the transporter and its subsequent degradation in lysosomes. In addition, we provide evidence that MT dynamics play a central role in the intracellular trafficking of the internalized transporter. Disintegration of the MT network by colchicine, as well as prevention of MT rearrangement by taxol, delays but does not persistently inhibit the trafficking from the subapical endocytic apparatus (SEA) to lysosomes. Downregulation of transport protein abundance through endocytosis and subsequent degradation, as demonstrated here for NaPi-2, may be a novel mechanism that also applies to other transport systems. It is noteworthy that our findings are based on an animal model that, in spite of its inherent limitations, supports the biological and physiological relevance of our data.

The downregulation of liganded receptors by RME is presently the best characterized endocytic mechanism. RME has been shown to be partially dependent on intact MTs (27). Depolymerization of MTs by antimitotic drugs such as nocodazole and colchicine interferes with degradation of endocytosed ligands. Presumably, the collapse of MTs results in the loss of directionality of vesicular transport from early to late endosomes and to lysosomes, whereby degradation becomes less efficient. Early events in RME that lead to internalization of receptor-ligand complexes into sorting endosomes are generally considered to be independent of MTs (28). Our morphological study of rapid downregulation of NaPi-2 in response to PTH suggests that trafficking of internalized NaPi-2 from a subapical endosomal compartment to juxtanuclear and more basal organelles is not only dependent on the integrity of MTs, but on their arrangement to dense MT bundles. The 2 lines of evidence that support this assumption are as follows: (a) the transient appearance of intracellular vesicles containing internalized NaPi-2 coincided temporally and spatially with the transient formation of MT bundles; and (b) taxol, which in our in vivo model prevented the transient formation of MT bundles, interfered with the trafficking and degradation of internalized NaPi-2.

In 1982, Herman and Albertini (29) reported a similar role of MT bundle formation in RME of cultured rat ovarian granulosa cells. This specific similarity between 2 distinct models — hormonally induced rapid endocytosis of a membrane transporter in vivo and ligand-induced RME in vitro — may indicate that the involvement of MT bundle formation is a general principle in rapid endocytosis.

According to a well-established concept, directional intracellular trafficking relies on motor-based translocation along MT tracks (28). The focusing of MTs in bundles on the endocytic pathway may thus increase the efficiency of vesicular traffic toward degradation. This focus may be of special significance in polarized epithelial cells, where MTs arise from MT organization centers in the apical periphery (23). If simple radial extension of MTs from their origin prevailed, endocytic traffic from the periphery along MTs could hardly converge toward central organelles.

Dynamic depolymerization and reformation of MTs is the basic principle of another, unorthodox model of MT-dependent trafficking, in which growing and shrinking MTs may directionally push or pull cargo attached to their fast-growing plus end. Whereas most data supporting this model were obtained from in vitro studies on mitotic movement of chromosomes (30), a

recent report by Blocker et al. (31) suggests that such a mechanism also plays a role in phagosome movement and might be extended to the trafficking of other membrane organelles, such as endocytic vesicles directed toward lysosomes.

The dependence of NaPi-2 downregulation on MTs is restricted to endocytic steps subsequent to the internalization of the transporter. Recent studies of NaPi-2 downregulation in response to a high dietary P_i load (4) had already shown that disruption of the microtubular cytoskeleton in PT cells by colchicine treatment of rats did not impair their capacity for rapidly internalizing NaPi-2. Correspondingly, the present study shows that neither disruption of MTs by colchicine nor impairment of their rearrangement by taxol hinder PTH-induced NaPi-2 internalization. However, the treatment with taxol has revealed the involvement of a subapical compartment in the early stages of NaPi-2 downregulation. Whereas at 15 minutes after PTH treatment, but in the absence of taxol, intracellular NaPi-2 tends to accumulate mainly in large vesicular organelles in the juxtanuclear and basal cell portion, the transporter seems to get transiently stuck in a distinct subapical region when rats have been pretreated with taxol. At a low incidence, this phenomenon is also observed in kidneys of rats treated solely with PTH or fed acutely with a high P_i diet (32), without prior taxol treatment. Hence, subapical accumulation of internalized NaPi-2 is not exclusively associated with the action of taxol. Rather, it is greatly enhanced by the antimitotic drug, facilitating the identification of subapical membrane structures that may participate in the trafficking of internalized transporter. Morphological examination with electron microscopy revealed that the subapical accumulation of NaPi-2 is accompanied by the appearance of large tubular membrane profiles. Considering their location and ultrastructural characteristics (see Results), we regard these profiles as the expanded form of so-called DATs of the SEA. Interestingly, Christensen and colleagues, who for years have been comprehensively studying the endocytic apparatus of PT cells, including the structure and function of DATs (24, 25), recently reported a very similar ultrastructural observation upon microinfusion of a particular cytological stain into PTs (33). In addition, they interpreted the appearance of numerous extended tubular membrane profiles in the subapical region as a strong increase in size and number of DATs, which was, as they reasoned, entailed by an inhibition of the intracellular endocytic pathway. The appearance of these large tubular membrane profiles thus may be considered the structural correlate of a deficiency in endocytic trafficking following the internalization of cargo into early endosomes. In our study, NaPi-2 protein likely is an essential component of this cargo, because its subapical accumulation coincided strictly with the apparent expansion of DATs. Presumably, when the uptake of retrieved NaPi-2 into the endosomal apparatus greatly exceeds the exit of sorted NaPi-2, as probably provoked by the MT-stabilizing agent taxol, the DATs may eventually become expanded.

The initial endocytic step, by which NaPi-2 is selectively removed from the BBM in response to PTH, remains to be characterized. Further morphological and functional studies on adequate models of experimental animals, isolated PTs, and cultured cells are required to clarify the endocytic mechanisms relevant for NaPi-2 downregulation.

In summary, the results from our study suggest that rapid downregulation of NaPi-2 in the BBM of renal PT cells in response to PTH occurs through endocytosis and degradation of the transporter. The endocytosis of NaPi-2 seems to proceed in 2 discrete steps. First, NaPi-2 is selectively retrieved from the apical membrane and is internalized into the SEA. This process is assumed to occur in an MT-independent manner. Second, internalized transporter exits the SEA and is directed to degradative organelles by MT-based trafficking. For high efficiency, this trafficking requires the rearrangement of MTs as mirrored by the formation of MT bundles along the degradation pathway. We hypothesize that NaPi-2 accumulates in the SEA, which eventually results in an expansion of DATs if the second endocytic step does not keep up with the first.

In addition, by revealing remarkable morphological alterations in the subapical region and the microtubular cytoskeleton, the present study suggests that upon a strong functional stimulus, rapid downregulation of NaPi-2 can arise to a major endocytic task of PT cells.

Acknowledgments

We thank Jan Loffing for valuable discussions. This work was supported by Swiss National Science Foundation grants 31-47742.96 (to B. Kaissling) and 31-46523.96 (to H. Murer), by grants from the DVA Merit Review and National Kidney Foundation (to M. Levi), and by a National Research Service Award (to H. Zajicek).

1. Murer, H., and Biber, J. 1997. A molecular view of proximal tubular inorganic phosphate (P_i) reabsorption and of its regulation. *Pflugers Arch.* **433**:379–389.
2. Levi, M., et al. 1994. Cellular mechanisms of acute and chronic adaptation of rat renal P_i transporter to alterations in dietary P_i. *Am. J. Physiol.* **267**:F900–F908.
3. Kempson, S.A., et al. 1995. Parathyroid hormone action on phosphate transporter mRNA and protein in rat renal proximal tubules. *Am. J. Physiol.* **268**:F784–F791.
4. Lötscher, M., Kaissling, B., Biber, J., Murer, H., and Levi, M. 1997. Role of microtubules in the rapid regulation of renal phosphate transport in response to acute alterations in dietary phosphate content. *J. Clin. Invest.* **99**:1302–1312.
5. Lötscher, M., et al. 1996. Regulation of rat renal Na/P_i-cotransporter by parathyroid hormone: immunohistochemistry [commentary]. *Kidney Int.* **49**:1010–1011.
6. Pfister, M.F., et al. 1997. Parathyroid hormone-dependent degradation of type II Na/P_i-cotransporters. *J. Biol. Chem.* **272**:20125–20130.
7. Pfister, M.F., et al. 1998. Lysosomal degradation of renal type II Na/Pi-cotransporter, a novel principle in the regulation of membrane transport. *Proc. Natl. Acad. Sci. USA.* **95**:1909–1914.
8. Keusch, I., et al. 1998. Parathyroid hormone and dietary phosphate provoke a lysosomal routing of the proximal tubular Na/P_i-cotransporter type II. *Kidney Int.* **54**:1224–1232.
9. Traebert, M., et al. 1999. Internalization of proximal tubular type II Na/Pi cotransporter by parathyroid hormone: an immunogold electron microscopy study. *Am. J. Physiol.* (In press.)
10. James, D.E., Strube, M., and Mueckler, M. 1989. Molecular cloning and characterization of an insulin-regulatable glucose transporter. *Nature.* **338**:83–87.
11. Fushimi, K., et al. 1993. Cloning and expression of apical membrane water channel of rat kidney collecting tubule. *Nature.* **361**:549–552.
12. Slot, J.W., Geuze, H.J., Gigengack, S., Lienhard, G.E., and James, D.E. 1991. Immunolocalization of the insulin-regulatable glucose transporter in brown adipose tissue of the rat. *J. Cell Biol.* **113**:123–135.
13. Katsura, T., et al. 1995. Constitutive and regulated membrane expression

of aquaporin 1 and 2 water channels in stably transfected LLC-PK1 epithelial cells. *Proc. Natl. Acad. Sci. USA.* **92**:7212–7216.
14. Marples, D., Knepper, M.A., Christensen, E.I., and Nielsen, S. 1995. Redistribution of aquaporin-2 water channels induced by vasopressin in rat kidney inner medullary collecting duct. *Am. J. Physiol.* **269**:C655–C664.
15. Sorkin, A., and Waters, C.M. 1993. Endocytosis of growth factor receptors. *Bioessays.* **15**:375–382.
16. Gruenberg, J., Griffiths, G., and Howell, K.E. 1989. Characterization of early endosomes and putative carrier vesicles in vivo and with an assay of vesicle fusion in vitro. *J. Cell Biol.* **108**:1301–1316.
17. Kochersberger, G., Bales, C., Lobaugh, B., and Lyles, K.W. 1990. Calcium supplementation lowers serum parathyroid hormone levels in elderly subjects. *J. Gerontol.* **45**:M159–M162.
18. Dawson, T.P., Gandhi, R., Le Hir, M., and Kaissling, B. 1989. Ecto-5′-nucleotidase: localization by light microscopic histochemistry and immunohistochemistry methods in the rat kidney. *J. Histochem. Cytochem.* **37**:39–47.
19. Levi, M., Jameson, D.M., and Van der Meer, B.W. 1989. Role of BBM lipid composition and fluidity in impaired renal P_i transport in aged rat. *Am. J. Physiol.* **256**:F85–F94.
20. Custer, M., Lötscher, M., Biber, J., Murer, H., and Kaissling, B. 1994. Expression of Na-P_i cotransport in rat kidney: localization by RT-PCR and immunohistochemistry. *Am. J. Physiol.* **266**:F767–F774.
21. Lötscher, M., et al. 1996. Immunolocalization of Na/SO_4-cotransport (NaSi-1) in rat kidney. *Pflugers Arch.* **432**:373–378.
22. Bloom, G.S., and Brashear, T.A. 1989. A novel 58-kDa protein associates with the Golgi apparatus and microtubules. *J. Biol. Chem.* **264**:16083–16092.
23. Bacallao, R., et al. 1989. The subcellular organization of Madin-Darby canine kidney cells during formation of a polarized epithelium. *J. Cell Biol.* **109**:2817–2832.
24. Christensen, E.I., and Nielsen, S. 1991. Structural and functional features in protein handling in the kidney proximal tubule. *Semin. Nephrol.* **11**:414–439.
25. Maunsbach, A.B., and Christensen, E.I. 1992. Functional ultrastructure of the proximal tubule. In *Handbook of physiology: renal physiology.* E.E. Windhager, editor. American Physiological Society. Washington, DC. 41–107.
26. Hatae, T., Ichimura, T., Ishida, T., and Sakurai, T. 1997. Apical tubular network in the rat kidney proximal tubule cells studied by thick-section and scanning electron microscopy. *Cell Tissue Res.* **288**:317–325.
27. Gruenberg, J., and Howell, K.E. 1989. Membrane traffic in endocytosis: insights from cell-free assays. *Annu. Rev. Cell Biol.* **5**:453–481.
28. Kelly, R.B. 1990. Microtubules, membrane traffic, and cell organization. *Cell.* **61**:5–7.
29. Herman, B., and Albertini, D.F. 1982. The intracellular movement of endocytic vesicles in cultured granulosa cells. *Cell Motil.* **2**:583–597.
30. Inoué, S., and Salmon, E.D. 1995. Force generation by microtubule assembly/disassembly in mitosis and related movements. *Mol. Biol. Cell.* **6**:1619–1640.
31. Blocker, A., Griffiths, G., Olivo, J.-C., Hyman, A.A., and Severin, F.F. 1998. A role of microtubule dynamics in phagosome movement. *J. Cell Sci.* **111**:303–312.
32. Ritthaler, T., et al. 1999. Effects of phosphate intake on distribution of type II Na/P_i cotransporter mRNA in rat kidney. *Kidney Int.* **55**:976–983.
33. Cui, S., Mata, L., Maunsbach, A.B., and Christensen, E.I. 1998. Ultrastructure of the vacuolar apparatus in the renal proximal tubule microinfused in vivo with the cytological stain light green. *Exp. Nephrol.* **6**:359–367.